1 **Characterization of *in vitro* engineered human adipose tissues: relevant adipokine**

2 **secretion and impact of TNF-α**

3

4 Kim Aubin [1, 2], Meryem Safoine [1, 2], Maryse Proulx [1, 2], Marie-Alice Audet-Casgrain [1], Jean-

5 François Côté [1], Félix-André Têtu [3], Alphonse Roy [4], Julie Fradette [1, 2, 5,*]

6

7 [1] Centre de recherche en organogénèse expérimentale de l'Université Laval / LOEX, Québec, Qc,

8 Canada

9 [2] Division of Regenerative Medicine, CHU de Québec Research Centre, Québec, Qc, Canada

10 [3] Clinique de chirurgie esthétique Félix-André Têtu and CHU de Québec, Québec, Qc, Canada

11 [4] Clinique de chirurgie plastique Alphonse Roy and CHU de Québec, Québec, Qc, Canada

12 [5] Department of Surgery, Faculty of Medicine, Université Laval, Québec, Qc, Canada

13 [*] Corresponding author

14 E-mail: Julie.fradette@chg.ulaval.ca (JF)

15 www.loex.qc.ca

16

17

18 Keywords: adipocytes, tissue engineering, self-assembly approach, adipose tissue, adipokine

19 secretion, TNF-α

20

21

Abstract

Representative modelling of human adipose tissue functions is central to metabolic research. Tridimensional models able to recreate human adipogenesis in a physiological tissue-like context *in vitro* are still scarce. We describe the engineering of white adipose tissues reconstructed from their cultured adipose-derived stromal precursor cells. We hypothesize that these reconstructed tissues can recapitulate key functions of AT under basal and pro-inflammatory conditions. These tissues, featuring human adipocytes surrounded by stroma, were stable and metabolically active in long-term cultures (at least 11 weeks). Secretion of major adipokines and growth factors by the reconstructed tissues was determined and compared to media conditioned by human native fat explants. Interestingly, the secretory profiles of the reconstructed adipose tissues indicated an abundant production of leptin, PAI-1 and angiopoietin-1 proteins, while higher HGF levels were detected for the human fat explants. We next demonstrated the responsiveness of the tissues to the pro-inflammatory stimulus TNF-α, as reflected by modulation of MCP-1, NGF and HGF secretion, while VEGF and leptin protein expression did not vary. TNF-α exposure induced changes in gene expression for adipocyte metabolism-associated mRNAs such as *SLC2A4*, *FASN* and *LIPE,* as well as for genes implicated in NF-κB activation. Finally, this model was customized to feature adipocytes representative of progressive stages of differentiation, thereby allowing investigations using newly differentiated or more mature adipocytes. In conclusion, we produced tridimensional tissues engineered *in vitro* that are able to recapitulate key characteristics of subcutaneous white adipose tissue. These tissues are produced from human cells and their neo-synthesized matrix elements without exogenous or synthetic biomaterials. Therefore, they represent unique tools to investigate the effects of pharmacologically active

43   products on human stromal cells, extracellular matrix and differentiated adipocytes, in addition to

44   compounds modulating adipogenesis from precursor cells.

45

Introduction

Adipose tissue (AT) is a highly active organ that regained particular attention considering its contributions to obesity-related dysfunctions such as insulin resistance and cardiovascular diseases [1-3]. In fact, white AT (WAT) predominates in humans, with distinct metabolic contributions of the visceral depots compared to the subcutaneous ones, especially under conditions of weight gain and obesity [4, 5]. In addition, recent descriptions of brown as well as beige/brite adipocytes in adults spurred a strong interest for these highly thermogenic cells of distinct developmental origin [6, 7]. WAT depots produce a great variety of active mediators that are secreted into the circulation, therefore impacting on many cell types and tissues [8]. Adipocytes, stromal cells and other resident cells (endothelial, immune cells, etc.) all contribute to AT secretome and functions, which are not restricted to fatty acid metabolism but also influence processes such as inflammation, immune modulation and angiogenesis [9, 10]. In particular, AT secreted factors such as leptin, plasminogen activator inhibitor-1 (PAI-1), angiopoietin-1 (Ang-1), vascular endothelial growth factor (VEGF) and hepatocyte growth factor (HGF) can impact vascular networks by acting on endothelial cell proliferation, migration and permeability. Ang-1 and PAI-1 are also known for their ability to influence capillary stability and the coordination between the adipogenic and angiogenic processes occurring during AT expansion [11-16].

Low-grade chronic inflammation characterizes the obese state and therefore, adipocytes are in contact with potent inflammatory mediators such as TNF-α (tumor necrosis factor α) and IL-1β (interleukin-1β) [17-19]. TNF-α affects many biological processes including differentiation, apoptosis and energy metabolism, in addition to modulating inflammation [3, 20]. Adipocytes are also producers of various interleukins such as IL-6, IL-8, IL-10 and IL-1β, therefore contributing

68   to the balance between pro- and anti-inflammatory networks [21, 22]. In fact, a novel research

69   area termed immunometabolism has emerged from the study of AT's roles in metabolism and

70   immunity, which contribute to the pathogenesis of obesity-associated dysfunctions [23, 24]. It is

71   of high importance to dissect adipose tissue responses during inflammation and pathological

72   situations. For such studies, the use of relevant human adipose tissue models engineered *in vitro*

73   could greatly contribute to the field.

74

75   Adipocytes develop from mesenchymal precursors through a coordinated adipogenic program

76   that was initially discovered using the immortalized rodent cultures 3T3-L1 and 3T3-F442A [25,

77   26]. This pioneering work established the molecular basis of adipogenesis, and differentiated

78   3T3-L1 and 3T3-F442A adipocytes are still widely used to study adipocyte metabolism

79   considering that they are easily cultured compared to the rather short-lived isolated primary

80   adipocytes or organotypic cultures [27, 28]. Of course, the human adipogenic program can also

81   be recapitulated using human mesenchymal precursors cells. In particular, the heterogeneous

82   stromal-vascular (SVF) fraction resulting from the enzymatic dissociation of subcutaneous AT

83   has been much studied for its therapeutic potential in recent years [29, 30]. This is due to the fact

84   that once plated and amplified in culture, adherent SVF cells are then called adipose-derived

85   stem/stromal cells *(*ASCs), which have been shown to contain not only preadipocytes but also a

86   subpopulation of stromal cells endowed with multilineage differentiation capacity including

87   neuronal cells, chondrocytes and osteoblasts [31, 32]. Moreover, an important part of the

88   therapeutic effects mediated by mesenchymal stem cells such as ASCs are associated with their

89   secretion of cytokines and growth factors promoting regenerative processes through cell

90   recruitment and proliferation while limiting apoptosis [33, 34].

91

92   Recent developments in the field of tissue engineering expanded the range of tridimensional (3D)

93   models available as research tools. Engineering of adipose tissue is mainly driven by the need to

94   develop human substitutes intended to restore soft tissue defects during reconstructive or

95   cosmetic procedures, given the variable long-term success rates of the current autologous fat

96   grafting procedures [35]. Due to their 3D structure, engineered adipose tissues also represent

97   excellent *in vitro* models for studying adipocytes under physiological or pathological conditions

98   since they usually feature a matrix-rich tissue-like context recapitulating the niche. Extracellular

99   matrix (ECM) components have proven to be essential for proper cell proliferation,

100 differentiation and signaling [36, 37]. Among models that are being developed for AT

101 engineering, the use of synthetic, biomimetic and natural matrices such as decellularized tissues

102 has been tested in conjunction with cells of various origin and species [38]. Our team has

103 previously shown that ASCs extracted from lipoaspirated fat can be expanded in culture and used

104 as building blocks for tissue engineering applications using the self-assembly approach. This

105 method consists of stimulating ECM production/deposition by the cells themselves with ascorbic

106 acid. By concomitantly inducing adipogenic differentiation *in vitro*, the resulting adipose cell

107 sheets feature numerous adipocytes as well as natural ECM components [39]. The production of

108 thicker tissues can be customized through the superposition of many cell sheets. In this study, our

109 goal was to determine if these *in vitro* human reconstructed adipose tissues (hrAT) could

110 recapitulate specific AT functions under basal conditions and in response to a pro-inflammatory

111 stimulus (TNF-α). To do so, we performed a detailed characterization of these hrAT samples.

112 The long-term maintenance and viability in culture of these adipose substitutes was assessed by

113 following adipocyte development and secreted factors production. Comparative data for leptin,

114 Ang-1, VEGF, PAI-1 and HGF release in conditioned media from hrAT as well as native human

115 AT explants provided information on the shared contribution of adipocytes and stromal cells to

116   the secretome. Finally, the responsiveness of the engineered tissues to the classic pro-

117   inflammatory cytokine TNF-α, both at the gene and protein expression levels, confirmed the

118   relevance of this 3D model as a novel tool to investigate biological responses of human WAT.

119

Materials and Methods

Ethics Statement

122   All studies involving human tissues and cells in culture were specifically approved by the Ethics

123   Committee of the CHU de Québec Research Centre (# DR-002-1117). Human subcutaneous AT

124   was obtained from non-obese men and women undergoing lipoaspiration or lipectomy

125   procedures, following their written informed consent for the use of these samples in research.

126

Tissues and culture systems

128   The characteristics of donors and AT samples used for organotypic cultures as well as for tissue

129   reconstruction are described in Table 1. Freshly harvested ATs were rinsed with phosphate-

130   buffered saline (PBS) solution containing antibiotics [100 U/ml penicillin (Sigma-Aldrich,

131   Oakville, ON, Canada) and 25 µg/ml gentamicin (Schering-Plough Canada Inc./Merck,

132   Scarborough, ON, Canada)]. Organotypic cultures were established by placing AT fragments

133   (average explants weight 851.6 mg, Table 1) in 24-well plates (VWR, Mississauga, ON, Canada)

134   containing 1.5 ml of complete adipocyte maintenance medium consisting of basal DMEM: F-12

135   (1:1) (DH) supplemented with 10 % fetal calf serum (FCS, HyClone, Logan, UT, USA), 100 nM

136   insulin (Sigma), 0.2 nM T3 (Sigma), 1 µM dexamethasone (Sigma) and antibiotics. Explants

137 were incubated for 48 h at 37°C in a humidified atmosphere containing 8 % CO_2. Controls for

138 protein quantification consisted of media alone incubated under the same conditions. Conditioned

139 media were harvested and frozen at -80°C until analysis. Explants were quick-frozen in liquid

140 nitrogen for DNA content determination. ASC cultures were established from lipoaspirates and

141 frozen at passage 0 according to a previously described methodology [39]. Cells were thawed and

142 expanded in DH medium supplemented with 10 % FCS and antibiotics.

143

144 **Table 1.** Description of AT used for organotypic cultures and/or tissue reconstruction
145

Population ID number	Age of donor	BMI of donor	Mean weight (mg)*	Number of samples (n)	Analyses performed on samples
AT explants					
1	32	23.3	610.0 (76.7)	6	Basal secretion
2	35	21.0	1807.7 (380.5)	3	Basal secretion
3 [#]	36	25.0	870.2 (136.2)	3	Basal secretion
4	38	20.1	467.4 (120.8)	6	Basal secretion
5 [&]	41	28.8	867.2 (70.1)	4	Basal secretion
6 [#, &]	55	25.3	486.9 (100.3)	6	Basal secretion
Mean (SD)	**39.5 (8.2)**	**23.9 (3.2)**	**851.6 (500.7)**	-	-
7	51	22.0	806.2 (123.8)	3	10 ng/ml TNF-α 24 h- treatment
	51	22.0	791.7 (52.0)	3	Control, non-treated samples
8	58	24.6	233.6 (35.0)	3	10 ng/ml TNF-α 24 h- treatment
	58	24.6	232.1 (11.1)	3	Control, non-treated samples
Mean (SD)	**54.5 (4.9)**	**23.3 (1.8)**	**515.9 (326.9**	-	-

Population ID number	Age of donor	BMI of donor	Mean weight (mg)* hrAT / hrCT	Number of samples (n) hrAT / hrCT	Analyses performed on samples
Reconstructed tissues (3.5 cm^2)					
3 [#]	36	25.0	30.1 (1.8) / 31.8 (1.3)	2 / 3	Basal secretion
6 [#, &]	55	25.3	29.6 (2.2) / 26.1 (0.5)	3 / 3	Basal secretion
9	38	29.5	28.1 (0.7) / 39.1 (0.9)	2 / 3	Basal secretion
10	54	24.9	26.3 (1.9) / 18.5 (1.7)	3 / 3	Basal secretion
Mean (SD)	**45.8 (10.1)**	**26.2 (2.2)**	**28.5 (1.7) / 28.9 (8.7)**	**-**	**-**

146 * : Values are indicated as mean (SD) when applicable.

147 & : indicates tissues from male donors

148 # : indicates data available for both AT explants and tissues reconstructed using the cells

149 extracted from adipose tissue from the same donor.

150

Production of reconstructed sheets and tissues

152 The self-assembly approach of tissue engineering was used to produce ASC-based connective or

153 adipose cell sheets [39]. After expansion, ASCs were seeded at passage 3 in DH medium

154 supplemented with 10 % FCS and antibiotics at a density of 1.56×10^4 cell/cm^2 in Nunc 6-well

155 plates (Thermo Fisher Scientific, Waltham, MA, USA) containing paper anchorage devices

156 (Whatman, Fisher Scientific, Ottawa, ON, Canada) to produce cell sheets of 3.5 cm^2 surface area.

157 Cultures were supplemented with ascorbic acid (AsA) (Sigma-Aldrich, Oakville, ON, Canada)

158 freshly prepared at each media change (every 2–3 days) and used at a concentration of 50 µg/ml

159 (250 µM) throughout the culture period. If not specified otherwise, adipogenic induction was

160 performed after 7 days of culture by using a defined cocktail containing 100 nM insulin (Sigma),

161   0.2 nM T3 (Sigma), 1 µM dexamethasone (Sigma), 0.25 mM 3-isobutyl-1-methylxanthine

162   (IBMX, Sigma) and 1 µM rosiglitazone (Cayman Chemical/Cedarlane, Burlington, ON, Canada)

163   in 3 % FCS-containing medium supplemented with AsA. After 3 days of induction, culture was

164   continued using complete adipocyte maintenance medium supplemented with AsA for the rest of

165   the culture period [39, 40]. In parallel, reconstructed connective sheets were produced from the

166   same ASC populations, by omitting the induction step (mock control media containing 3 % FCS

167   and 0.038 % dimethyl sulfoxide) and further culturing in 10 % FCS DH medium (with AsA and

168   antibiotics). After 28 days of culture, thicker human reconstructed connective tissues (hrCT) and

169   hrAT were produced by the superposition of three individual cell sheets, and further cultured for

170   at least 7 days before being harvested for analyses. Finally, an additional protocol for the

171   engineering of hrAT was evaluated in order to obtain adipocytes at specific stages of

172   differentiation. Static cultures were compared to dynamic culture conditions created by a 3D

173   shaker platform gyrating at 35 rpm (GyroTwister™ and Ocelot Rotator, Fisher Scientific)

174   inducing a wave-like motion of the medium throughout the culture period [41]. For that study,

175   adipogenic induction was performed either after 7, 14 or 21 days of culture with AsA and cell

176   sheets were superposed at day 28 to create thicker tissues.

177

178   Histological analyses and adipocyte surface area measurements

179   Samples of native and reconstructed AT (three layers-thick) were formalin-fixed and paraffin

180   embedded. Cross sections (5 µm) were stained with Masson's trichrome and pictures taken using

181   a microscope Nikon Eclipse Ts100 equipped with a Nikon Coolpix 4500 camera (Nikon,

182   Montreal, Qc, Canada). Histology micrographs were analyzed to determine the mean area (μm^2)

183   occupied by individual adipocytes on tissue sections using a semi-automated protocol outlining

184   adipocyte contours (Simple PCI software, Hamamatsu Corporation, Bridgewater, NJ). The

185   number of adipocytes per μm^2 of tissue and their surface area were determined in order to

186   generate mean values and frequency distribution graphs for each time-point examined. On

187   average, more than 900 adipocytes were measured for each sample (n = 3-4) at each time-point.

188

Immunolabelings and imaging of whole mount tissues

190   Confocal imaging on whole mount samples of reconstructed (56 days of culture/49 days of

191   differentiation) and native AT obtained from lipectomy procedures (37 and 51 year-old donors,

192   BMI < 25) were performed using modifications of previously described methods [42]. Briefly, ~

193   8 mm^3 free-floating formalin-fixed samples were washed in 1 % w/v bovine serum albumin

194   (BSA, Sigma) in PBS before incubation at 4°C for 48 h with either a polyclonal rabbit anti-

195   human collagen type IV primary antibody (Ab6586 (GR696641), 2.5 µg/ml, Abcam inc, Toronto,

196   ON, Canada) or polyclonal rabbit IgG (AB-105-C (ER1211041), 2.5 µg/ml, R&D systems,

197   Minneapolis, MN, USA) as negative control. Samples were then incubated in a 1 % PBS-BSA

198   solution containing goat anti-rabbit IgG-coupled Alexa633 secondary antibody (A-21071

199   (1073050), 5 µg/ml, Molecular Probes) for 72 h at 4°C. In order to visualize the lipid content of

200   formalin-fixed AT samples, incubation for a minimum of 2 h was performed in a 200 ng/ml Nile

201   Red solution (N-1142 (0151-12), Life technologies, Burlington, ON, Canada). Images were

202   acquired using a Zeiss LSM700 scanning laser confocal microscope and image software (2011,

203   Carl Zeiss MicroImaging GmbH, Jena, Germany). They were processed using the Zen software

204   (Zeiss) to obtain two-dimensional (2-D) representations of initial 3-D images by applying a

205   ''Maximum Intensity Projection'' method [42].

206

Scanning electron microscopy (SEM)

Tissue samples were fixed with 1.25 % glutaraldehyde/2 % paraformaldehyde in 0.1 M

cacodylate buffer for 24 h before being processed with hexamethyldisilazan followed by gold-

palladium coating. All micrographs were obtained at 30 kV on a JEOL 6360LV SEM microscope

(Tokyo, Japan).

TNF-α treatments

Lyophilized recombinant human TNF-α (EMD Millipore (Merck) /Cedarlane, Burlington, ON,

Canada) was reconstituted in water, aliquoted and stored at -20°C. At the time of treatment, serial

dilutions were prepared and added to the wells at a final concentration of 10 or 100 ng/ml TNF-α.

Human reconstructed connective and adipose sheets (27 days of adipogenic differentiation) were

assessed in triplicate from one (6 h, 72 h) or two distinct experiments (24 h, two different cell

populations). Twenty-four hours before the treatment, the cultures were changed to DH medium

supplemented with 10 % FCS and antibiotics. Connective and adipose sheets were incubated with

TNF-α for specified concentrations and durations before being harvested, washed in PBS, quick-

frozen in liquid nitrogen and stored at -80°C for mRNA analysis. Conditioned media were also

harvested at indicated time-points and stored at -80°C for analysis. For explants, AT fragments

obtained after lipectomy procedures (average weight 515.9 mg, Table 1) were exposed or not to

10 ng/ml of TNF-α for 24 h in 24-well plates containing 1.0 ml of adipocyte maintenance

medium devoid of dexamethasone. Explants were incubated at 37°C in a humidified atmosphere

containing 8 % CO_2. Controls for protein quantification consisted of media alone incubated under

the same conditions. Conditioned media were harvested and frozen at -80°C until analysis.

Quantitative Real-Time PCR method

230

231   Total RNAs were isolated from engineered cell sheets treated with TNF-α (10 or 100 ng/ml) or

232   their correspondent control media for 6 h (n = 3), 24 h (n = 6, 2 distinct experiments) or 72 h (n =

233   3). Tissues were homogenized in Qiazol buffer (Qiagen, Germantown, MD, USA) and total RNA

234   was extracted using the RNeasy mini kit on-column DNase (Qiagen, Hilden, Germany) treatment

235   following the manufacturer's instructions. Quantity of total RNA was measured using a

236   NanoDrop ND-1000 Spectrophotometer (NanoDrop Technologies, Wilmington, DE, USA) and

237   total RNA quality was assayed on an Agilent BioAnalyzer 2100 (Agilent Technologies, Santa

238   Clara, CA, USA). First-strand cDNA synthesis was accomplished using 2.8-4.5 µg of isolated

239   RNA in a reaction containing 200 U of Superscript III Rnase H-RT (Invitrogen Life

240   Technologies, Burlington, ON, Canada), 300 ng of oligo-dT$_{18}$, 50 ng of random hexamers, 50

241   mM Tris-HCl pH 8.3, 75 mM KCl, 3 mM MgCl$_2$, 500 µM deoxynucleotides triphosphate, 5 mM

242   dithiothreitol, and 40 U of Protector RNase inhibitor (Roche Diagnostics, Indianapolis, IN, USA)

243   in a final volume of 50 µl. Reaction was incubated at 25°C for 10 min, then at 50°C for 1 h and

244   PCR purification kit (Qiagen) was used to purify cDNA.

245

246   Oligoprimer pairs were designed by GeneTool 2.0 software (Biotools Inc, Edmonton, AB,

247   Canada) and their specificity was verified by blast in the GenBank database. The synthesis was

248   performed by IDT (Integrated DNA Technology, Coralville, IA, USA) (Table 2). cDNA

249   corresponding to 20 ng of total RNA was used to perform fluorescent-based Realtime PCR

250   quantification using the LightCycler 480 (Roche Diagnostics, Mannheim, Germany). Reagent

251   LightCycler 480 SYBRGreen I Master (Roche Diagnostics, Indianapolis, IN, USA) was used as

252   described by the manufacturer with 2 % DMSO. The conditions for PCR reactions were: 45

253 cycles, denaturation at 95°C for 10 sec, annealing at 57-62°C for 10 sec, elongation at 72°C for

254 14 sec and then 74°C for 5 sec (reading). A melting curve was performed to assess non-specific

255 signal. Calculation of the number of copies of each mRNA was performed according to Luu-The

256 et al., using a second derivative method and a standard curve of Cp versus logarithm of the

257 quantity [43]. The standard curve was established using known amounts of purified PCR

258 products (10, 10^2, 10^3, 10^4, 10^5 and 10^6 copies) and a LightCycler 480 v1.5 program provided by

259 the manufacturer (Roche Diagnostics). PCR amplification efficiency was verified. Normalization

260 was performed using the geometric mean data from three reference genes shown to be genes

261 having stable expression levels in adipose-derived stem cells and adipose tissue: glucuronidase,

262 beta (GUSB), ubiquitin C (UBC), TATA box binding protein (TBP) [44]. Quantitative Real-Time

263 PCR measurements were performed by the CHU de Québec Research Center (CHUL) Gene

264 Expression Platform, Québec, Canada and were compliant with MIQE guidelines [45].

265

266 **Table 2**. Primer sequences and gene description

Gene Symbol	Description	GenBank	size (pb)	Primer sequence 5'→3' S/AS
CCL2	Homo sapiens chemokine (C-C motif) ligand 2 (CCL2)	NM_002982	188	GCAGCCACCTTCATTCCCCAA/ GCACAGATCTCCTTGGCCACA
SLC2A4	Homo sapiens solute carrier family 2 (facilitated glucose transporter), member 4 (SLC2A4)	NM_001042	212	CCAGTATGTTGCGGAGGCTAT/ CGTTCTCATCTGGCCCTAAATA CT
LIPE	Homo sapiens lipase, hormone-sensitive (LIPE)	NM_005357	191	GAAGACTCTGCAGGGATCCAA TA/TTTGGATGTAAGGTGATTG CTGTGG

FASN	Homo sapiens fatty acid synthase (FASN)	NM_004104	257	TGCGTGGCCTTTGAAATGTGCT/ACACGCTCCTCTAGGCCCTTCA
NFKB1	Homo sapiens nuclear factor of kappa light polypeptide gene enhancer in B-cells 1 (NFKB1), 2 transcripts	NM_003998	180	AGCCTCTCTATGACCTGGATGACT/GCTGTTTCATGTCTCCTTGTGCTAGT
NFKB2	Homo sapiens nuclear factor of kappa light polypeptide gene enhancer in B-cells 2 (p49/p100) (NFKB2), 4 transcripts	NM_00107794	256	ACGAACAGCCTTGCATCTAGCC/CCCTTCAGAGTCCGAGTCGCT
NFKBIA	Homo sapiens nuclear factor of kappa light polypeptide gene enhancer in B-cells inhibitor, alpha (NFKBIA)	NM_020529	143	TACCTGGGCATCGTGGAGCTT/TCAGCCCCACACTTCAACAGGA
IKBKB	Homo sapiens inhibitor of kappa light polypeptide gene enhancer in B-cells, kinase beta (IKBKB), 8 transcripts	NM_001556	215	GCCGTGAGAAAAGTGCTTGGAG/GGCCGCAACTATAATTAAACTGTCTG
TRAF1	Homo sapiens TNF receptor-associated factor 1 (TRAF1), 3 transcripts	NM_005658	244	AACCCATCTGTCGCTCTTCATC/GTAGGCGTGCTTGGGTGACTG
TNFAIP3	Homo sapiens tumor necrosis factor, alpha-induced protein 3 (TNFAIP3), 3 transcripts	NM_00127050 8	241	GGCCTCTTTGATACACTTTTGCT/ACCATCACAAAAGGCCACATCT
BIRC3	Homo sapiens baculoviral IAP repeat containing 3 (BIRC3), 2 transcripts	NM_001165	171	TTCATCCGTCAAGTTCAAGCCAGT/CACGGCAGCATTAATCACAGGA
BCL2	Homo sapiens B-cell CLL/lymphoma 2 (BCL2), 2 transcripts	NM_000633	98	GGTGGGGGTCATGTGTGTGGAGAG/TGCAGGTGCCGGTTCAGGTACT

JUN	Homo sapiens jun proto-oncogene (JUN)	NM_002228	229	CGGCCAACATGCTCAGGGAAC /ACCCTTGGCTTTAGTTCTCGG ACAC
UBC	Homo sapiens ubiquitin C (UBC)	NM_021009	127	CTCGGCCTTAGAACCCCAGTA/ AGAATCGCCGAGAAGGGACTA C
GUSB	Homo sapiens glucuronidase, beta (GUSB)	NM_000181	130	CGACGAGAGTGCTGGGGAATA /TTGGCTACTGAGTGGGGATAC CT
TBP	Homo sapiens TATA box binding protein (TBP), 2 transcripts	NM_003194	189	CGGGCACCACTCCACTGTATC/ GCTTGGGATTATATTCGGCGTT TC
gDNA (Control)	Homo sapiens 3-beta-hydroxysteroid dehydrogenase/delta-5-delta-4-isomerase (3-beta-HSD) gene (intron)	M38180	260	GAAGGGCAGAGGTGGAACTA GAA/AACAAAGACCAAAGACC AGTGAGA

267

Adipokine quantification by ELISA assays

269 Complete culture media conditioned for 48 h by connective or adipose cell sheets were harvested

270 each week during 7 weeks and stored at -80°C before Ang-1 analyses (Duoset®, R&D systems).

271 Results are presented for cells originating from three different donors and are expressed as ng/ml

272 ± standard deviation (SD). Also, connective cell sheets or adipose sheets featuring adipocytes

273 differentiated for 28 days were treated or not with 10 or 100 ng/ml of TNF-α for 24 h.

274 Conditioned media (n = 6 per experimental group, mean ± SD) were analyzed for MCP-1

275 (Duoset® ELISA, R&D systems), free NGF (Emax® ImmunoAssay Systems, Promega,

276 Madison, WI, USA), HGF, VEGF and leptin (all DuoSet® from R&D systems). For the

277   comparative study of the secretion profiles, media conditioned by AT explants, hrCT and hrAT

278   (detailed in Table 1) were harvested and frozen at -80°C until analysis. Leptin, Ang-1, VEGF,

279   PAI-1 (DuoSet®, R&D systems) and HGF levels were then quantified. Reconstructed tissues

280   cultured for 35 days (hrCT) and 28 days of adipogenic differentiation (hrAT) were used and their

281   supernatants harvested by collecting the complete serum-containing 48 h-conditioned media (20-

282   22 ml). Finally, for each molecule and experiment, controls were performed by incubating the

283   appropriate media in absence of cells, and if applicable, by subtracting the baseline levels from

284   data.

285

286   ## Determination of DNA content

287   In order to account for the different weights and cellularity of AT explants compared to hrAT,

288   data normalization was performed using total DNA content of the corresponding AT explants.

289   For hrCT and hrAT, tissues reconstructed from 4 cell populations (N = 4, n = 2-3) were

290   used for paired data normalization. DNA content was determined using the Quant-iT™

291   PicoGreen® dsDNA Assay Kit (Life Technologies). Briefly, tissues were digested overnight at

292   56°C in 10 % Proteinase K solution (Qiagen). The remaining lipid phase was discarded and the

293   aqueous phase was treated with RNAse A (Life Technologies) for 2 h. As per manufacturer

294   instructions, the Picogreen® reagent was added to diluted samples and $_\lambda$DNA standards and

295   incubated for 5 minutes before reading (Excitation: 485 nm; Emission: 520 nm) using a

296   Varioskan Flash multimode reader (Thermo Electron Corporation) and SkanIt RE for Varioskan

297   Flash 2.4.3 software.

298

299   ## Oil Red O staining and lipid quantification

300   Adipose cell sheet engineering was performed as detailed above in presence or not of the wave-

301   like movement (GyroTwister™ and Ocelot Rotator, Fisher Scientific). Lipid quantification was

302   performed as previously described [39] on adipose cell sheets that were induced to differentiate

303   into adipocytes at d7, d14 and d21 of culture, and further cultured for a fixed period of 14 days of

304   differentiation. The corresponding connective sheets engineered from the same cells without

305   adipogenic induction and cultured for the same amount of time were used as controls. Results are

306   expressed as relative units corresponding to the mean of the ORO values (± standard error of the

307   mean, SEM) obtained for the cultures induced with the adipogenic cocktail in reference to the

308   OD reading of the non-induced cultures. Seven distinct experiments were performed using cells

309   from 4 different donors. Each experiment was performed in triplicate. Oil red O staining was also

310   performed on transverse cryosections (20 μm) of formalin-fixed tissues embedded in optimal-

311   cutting temperature (OCT) compound. Staining of the tissues for 15 min was followed by rinsing

312   in PBS buffer before photographs being taken with a Nikon Eclipse Ts100 microscope with a

313   Nikon Coolpix 4500 camera.

314

315   Statistical analyses

316   Data are expressed as mean ± SD for representative experiments, and as mean ± SEM when

317   presenting results pooled from multiple experiments/donors. Statistical comparisons were made

318   using the GraphPad Prism 6 software (GraphPad Software Inc., La Jolla, CA, USA) and are

319   specified in the figure legends (one-way analysis of variance (ANOVA), one-sample t-tests or

320   unpaired t-tests). The confidence interval was set at 95 % ($P \leq 0.05$).

321

322   Results

Reconstruction of metabolically active human adipose tissue

Highly natural and manipulatable hrAT were produced *in vitro*. They exhibited features of human

WAT at the histological (Fig 1A, B, C) and scanning electron microscopy (SEM) levels (Fig 1E).

Masson's trichrome staining was performed on sections of paraffin-embedded reconstructed

tissues maintained in culture for up to 88 days. Adipogenic induction was performed after 7 days

of culture with AsA-containing medium, and adipocyte differentiation was allowed to progress

for 28 (Fig 1A), 49 (Fig 1B) and 81 days (Fig 1C), respectively. Histological cross-sections

reveal numerous adipocytes (void spaces) embedded into the cell-derived ECM (in blue). The

latter is more homogenously distributed within hrAT than for native AT (Fig 1D), for which

adipocytes are arranged into fat lobules supported by dispersed ECM-rich stroma. Low

magnification overview by SEM highlights the varied range in diameter of the *in vitro*

differentiated adipocytes of the reconstructed tissue (Fig 1E), as well as the cell sheet structure

(Fig 1E, arrow). A similar topology was observed for AT samples that features a greater

proportion of larger adipocytes (Fig 1F). The lipid content of the adipocytes is revealed after

staining with Nile Red dye (Fig 1G, H). Adipocytes are surrounded by a basement membrane

containing collagen type IV, both for reconstructed (Fig 1I) and native AT (Fig 1J). Collagen

type IV is also present in the basement membrane of blood vessels of native AT samples (Fig 1J,

asterisk).

Fig 1. Morphological features of hrAT. The structural appearance of the hrAT engineered *in*

vitro is revealed on tissue cross-sections after Masson's trichrome staining. (A-C) Numerous

adipocytes embedded in ECM can be distinguished within tissues submitted to adipogenic

induction after 7 days of culture and differentiated for (A) 28, (B) 49 and (C) 81 days. (D)

346 Histology of human native subcutaneous AT from a 54 year-old donor. (E) Scanning electron

347 microscopy exposes rounded adipocytes (25 days of differentiation) in the matrix-rich hrAT. The

348 arrow points to a region of the hrAT revealing the sheet-like structure. (F) Appearance by SEM

349 of adipocytes from a 58 year-old donor. Lipids within adipocytes from (G) hrAT and (H) AT

350 samples can be observed after Nile Red staining. Staining for collagen type IV on (I) hrAT and

351 (J) native AT reveals its localization in basement membranes. (K) and (L) represent isotype

352 antibody controls for labeling of hrAT and native AT, respectively. Asterisk (*): blood capillary.

353

354 The hrAT produced were not only structurally stable over a long culture period but were

355 continuously metabolically active and responsive to the culture environment. This is supported by

356 the mean adipocyte size increase over time in culture (Fig 2A), as measured from adipocyte

357 surface area on histological cross-sections, reflecting the progressive accumulation of lipid

358 droplets. In particular, frequency distribution graphs indicate a gradual decrease in the number of

359 adipocytes featuring smaller surface areas at both 49 days and 81 days of adipogenic

360 differentiation, while larger adipocytes of 350 -1 500 μm^2 increased almost 4.5 times at the end

361 of the culture period, namely 81 days after adipogenic induction (Fig 2B). In addition to this

362 capacity to expand in size and store triglycerides, adipocytes within the reconstructed tissues

363 actively secreted bioactive molecules. Increasing amounts of the angiogenic modulator Ang-1

364 (Fig 2C) were quantified in the media conditioned by the reconstructed sheets along with

365 adipocyte development (up to 42 days of differentiation). Connective sheets produced from the

366 same cells without adipogenic induction produced lower levels of Ang-1 at each time-point (Fig

367 2C), indicating a contribution of undifferentiated stromal cells to the Ang-1 levels produced by

368 adipose sheets.

369

370 **Fig 2. Long-term stability of the hrAT *in vitro*.** (A) Mean surface area of the adipocytes over

371 the culture period as measured from histological sections of hrAT harvested after 28, 49 or 81

372 days of *in vitro* differentiation. (B) Frequency distribution of adipocyte cell surface area

373 according to the number of days the tissues were maintained in culture after adipogenic

374 induction. Mean ± SEM. One-way ANOVA followed by Tukey's post-hoc tests were performed

375 and the significance is indicated in reference to day 28 (*) or day 49 (#). ***$P \leq 0.001$, **$P \leq 0.01$,

376 * and # $P \leq 0.05$. (C) Kinetics of Ang-1 secretion in media conditioned by reconstructed cell sheets

377 maintained in culture up to 49 days. Connective sheets were produced using the same cells as

378 adipose sheets but without the adipogenic induction step. Results are expressed as ng/ml/48 h per

379 sheet of 3.5 cm^2. Data from cell sheets engineered from three distinct cell populations is

380 represented (N = 3, n = 2-3 for each time-point). Mean ± SD, # indicates statistical difference

381 between connective and adipose sheets at each time-point ($P \leq 0.05$, unpaired *t*-tests) while

382 asterisks (*) indicate the comparison between consecutive weeks within the same cell population.

383 & indicates that all three populations are significantly different between consecutive weeks. One-

384 way ANOVA followed by Tukey's post-hoc test. **** $P \leq 0.0001$, *** $P \leq 0.001$, **$P \leq 0.01$, * and

385 & $P \leq 0.05$.

386

Main secretory products detected in the conditioned media: a comparison with AT explants

389 We then assessed the secretion of the major adipokine leptin as well as a range of molecules

390 (VEGF, Ang-1, HGF, PAI-1) reflecting the physiological functions mediated by AT such as the

391 modulation of angiogenic processes. We quantified these molecules in the conditioned media of

392 reconstructed tissues featuring adipocytes differentiated for 28 days in comparison to human AT

393   explants maintained in complete adipocyte maintenance medium for 2 days after AT harvest (Fig

394   3 and Table 1). Data was normalized using total DNA content (Fig 3F) since weight and

395   cellularity varied among samples, donors and tissue types. Measured amounts of leptin (Fig 3A)

396   and PAI-1 (Fig 3B) were within the same order of magnitude between hrAT and AT explants.

397   Higher levels of the pro-angiogenic factors Ang-1 (Fig 3C, 6.2-fold) and VEGF (Fig 3D) were

398   noted in hrAT. In fact, almost negligible amounts of VEGF were detected in the media

399   conditioned by the AT explants. Finally, HGF levels (Fig 3E) were more pronounced for AT

400   explants than for hrAT or hrCT. The secretion profiles of the undifferentiated stromal cells within

401   hrCT were also established and compared to hrAT reconstructed from the same ASC populations.

402   On average, these connective tissues secreted comparable amounts of HGF, slightly higher

403   amounts of VEGF (up to 3.9-fold), but lower levels of PAI-1 (2.3-fold, t-test, $P = 0.0025$) and

404   Ang-1 (2.4-fold) than hrAT.

405

406   **Fig 3. Secretion of key adipokines by AT explants and reconstructed tissues.** Culture media

407   conditioned for 48 h by AT explants (N = 6 donors, n = 3-6 per donor) as well as hrAT (28 days

408   of differentiation) and their hrCT undifferentiated counterparts (N = 4, n = 2-3) were analyzed by

409   ELISA assays. Secreted levels of (A) leptin, (B) PAI-1, (C) Ang-1, (D) VEGF and (E) HGF were

410   determined. Data are expressed as pg/ml of molecule secreted in 48 h normalized by total DNA

411   content (means ± SEM). Each datapoint represents the mean value obtained for many samples

412   derived from a distinct donor/population (Table 1). (F) Total DNA content determination. One-

413   way ANOVA followed by Tukey's post-hoc test. ***$P \leq 0.001$, **$P \leq 0.01$, *$P \leq 0.05$. ND = not

414   detected.

415

Modulating the functional responses within engineered tissues

Adipocytes are influenced by the specific microenvironment they are sensing. Their biological responses can be modulated by external stimuli such as the pro-inflammatory cytokines TNF-α and IL-1β. We probed the *in vitro* responsiveness of the reconstructed adipose sheets to TNF-α by monitoring gene expression in the tissues and assessing important secreted factors in conditioned media. Expression of both TNF-α receptors was detected at the mRNA level (Table 3), with higher expression level of *TNFRSF1A* in comparison to *TNFRSF1B* (14-fold). *TNFRSF1A* expression was slightly decreased by TNF-α, while the expression level of *TNFRSF1B* was significantly increased (up to 3.8-fold) in presence of TNF-α (Table 3).

Dosage-dependent changes in the secretory capacity of adipose cell sheets were assessed for the production of monocyte chemoattractant protein 1 (MCP-1) which has an important role for immune cell recruitment at the site of inflammation *in vivo*. Increased MCP-1 secretion was detected in conditioned media 24 h after stimulation with 10 and 100 ng/ml TNF-α (Fig 4A). Additional cytokines and growth factors reportedly influenced by or mediating TNF-α actions were also evaluated (Fig 4B). As seen for MCP-1, a significant increase of free NGF (1.6- and 2.3-fold) and HGF (1.6- and 1.5-fold) proteins were observed after a 24 h stimulation at both 10 and 100 ng/ml TNF-α concentrations, respectively. However, the basal levels of VEGF and leptin detected in those conditioned media did not vary upon TNF-α exposure (Fig 4B). In parallel, connective cell sheets were also exposed to TNF-α, and the stromal cells forming these tissues responded by an increased MCP-1 secretion (Fig 4C, 2 to 3-fold) and a slightly increased HGF secretion (1.2-fold), while VEGF did not vary. When the amounts (ng/ml) of these molecules secreted by connective and adipose sheets are compared (Fig 4D), the important contribution of

439 stromal cells of the connective sheets can be observed, both in absence and presence of

440 exogenous TNF-α, when compared to adipose sheets (comprising adipocytes and remaining

441 stromal cells that did not differentiate into adipocytes). Finally, the cellular responses of AT

442 explants to TNF-α was also investigated (Fig 4E), revealing a profile similar to those of the

443 reconstructed tissues (Fig 4B) including the modulation of MCP-1 (3.8-fold) but no change in

444 VEGF or leptin secretion. HGF secretion was not significantly modified by 10 ng/ml TNF-α in

445 these AT explants (Fig 4E).

446

447 **Table 3. Gene expression in adipose sheets is modulated by TNF-α exposure**

Gene symbol	Fold variation over control [#]					
Treatment duration	6 h		24 h		72 h	
[TNF] (ng/ml)	**10**	**100**	**10**	**100**	**10**	**100**
TNFRSF1A	-1.1 *	-1.1 *	-1.2 **	-1.2 ****	-1.0	-1.2 ***
TNFRSF1B	2.3 **	2.6 *	1.7 ****	2.0 ****	1.8 ***	3.8 **
CCL2	9.8 **	8.7 ***	4.4 **	9.6 ****	2.3 *	4.4
SLC2A4	-1.3 *	-1.3 *	-2.2 **	-2.5 ***	1.0	-1.4 *
FASN	-1.6 *	-1.5 *	-1.7 **	-2.1 ***	1.0	-2.8 ***
LIPE	-2.2 **	-3.2 ***	-1.8 **	-2.8 ****	-1.5	-3.2 **
PTGES	3.5	3.9	4.1	5.4	1.1	3.3

	**	***	**	***		**
PTGES2	-1.0	1.2 ****	1.0	1.1	-1.1	1.1
PTGES3	1.1	1.1	1.1 **	1.2 ***	1.2	1.3 *
NFKB1	7.3 **	7.8 **	2.3 ***	3.3 ****	1.5 ***	3.4 **
NFKB2	7.3 ***	9.3 **	3.6 **	5.8 ****	1.5 ***	4.8 ***
IKBKB	1.7 ***	1.7 *	1.2 *	1.3 ****	1.0	1.2 *
NFKBIA	9.5 ***	12.7 **	4.9 **	9.7 ****	1.8 *	8.6 **
BIRC3	37.1 **	38.7 ***	15.8 ***	34.6 ****	3.0 ***	28.6 **
TNFAIP3	25.3 ***	35.3 **	13.4 *	29.7 ****	2.4 **	25.6 **
PTGS2	12.2 **	21.7 **	-1.1	3.4 ***	-1.3 **	1.4
TRAF1	10.0 **	15.0 **	2.9 **	5.6 ****	1.3 ***	10.5 *
JUN	3.0 **	3.3 **	1.2	2.1 ****	1.3	2.3 **

448 (-) indicates a decrease in expression.

449 <superscript>#</superscript> Statistical analyses were performed for each time-point using one-sample *t*-tests comparing fold

450 variation ratio of each TNF-α condition to the untreated controls (value of 1). (****P≤0.0001,

451 ***P≤0.001, **P≤0.01, *P≤0.05).

452

453 **Fig 4. Effects of TNF-α on adipokine secretion by reconstructed tissues and AT explants.**

454 (A) Dose-dependent release of MCP-1 after exposure to TNF-α. Adipose cell sheets were

455 incubated for 24 h in presence of 10 or 100 ng/ml of TNF-α and the conditioned media were

456 analyzed by ELISA assays. One-way ANOVA followed by Tukey's post-hoc test. ***P≤0.001

457 compared to control, <superscript>##</superscript>P≤0.01 compared to 10 ng/ml TNF-α. (B) Fold increase protein

458 expression over control for MCP-1, free NGF, HGF, VEGF and leptin following a 24 h

459 exposition of adipose sheets to 10 or 100 ng/ml TNF-α. (C) Fold increase protein expression over

460 control for MCP-1, HGF and VEGF following a 24 h exposition of connective sheets to 10 or

461 100 ng/ml TNF-α. For each molecule, one-sample *t*-tests were performed in reference to

462 untreated sheets (ratio of 1). For B and C, One-way ANOVA followed by Dunnett's post-hoc test

463 ****P≤0.0001, ***P≤0.001, **P≤0.01. (D) Comparative amounts (ng/ml) of MCP-1, HGF and

464 VEGF secreted by the connective and adipose cell sheets following a 24 h exposure to 10 ng/ml

465 TNF-α. Dashed lines within each column indicate the basal level of mock-treated connective and

466 adipose sheets for the corresponding secreted protein. # indicates statistical significance for these

467 basal levels between connective and adipose sheets while asterisks (*) indicate significance

468 between tissue types. ****P≤0.0001, **P≤0.01, *P≤0.05. Note that leptin is not produced by

469 connective sheets or hrCT. (E) Fold increase protein expression over control for MCP-1, HGF,

470 VEGF and leptin following a 24 h exposition of human AT explants to 10 ng/ml TNF-α. Data

471 normalization was performed according to the weight of the explants.

472

TNF-α mediated modulation of gene expression

474 The earlier (6 h) and prolonged (24 h, 72 h) effects of TNF-α on gene expression of human

475 adipocyte-abundant genes as well as on members/target genes of the NF-κB activation pathway

476 were also examined (Table 3). Genes coding for MCP-1 (*CCL2*) as well as the metabolically

477 relevant proteins facilitated glucose transporter 4 (Glut-4, *SLC2A4*), fatty acid synthase (FAS,

478 *FASN*) and hormone-sensitive lipase (HSL, *LIPE*) were evaluated after exposure to 10 and 100

479 ng/ml TNF-α. Such stimulation led to up to 10-fold increases in gene expression for *CCL2* in

480 adipose cell sheets after 6 h and 24 h (Table 3). In contrast, *SLC2A4, FASN* and *LIPE* were

481 significantly downregulated, in particular at 100 ng/ml of TNF-α at all time-points examined

482 (Table 3).

483 The prostaglandin E synthases (*PTGES*, *PTGES2*, *PTGES3*) gene expression levels were also

484 assessed after TNF-α exposure. While a moderate increase (up to 5-fold) of *PTGES* was

485 generally observed in presence of TNF-α, none to slight modulations (up to 1.3-fold) were

486 detected for *PTGES2* and *PTGES3*. In addition, mRNAs encoding two DNA-binding subunits of

487 NF-κB (*NFKB1* and *NFKB2*) were induced by TNF-α, presenting significant increases at all

488 time-points with a more pronounced effect after 6 h (8- and 9-fold respectively) and decreasing

489 afterwards. A much lower increase (1.2- to 1.7-fold) was observed for the IKK-β (*IKBKB*)

490 member of the IκB kinase superfamily at 6 and 24 h for both concentrations, while only 100

491 ng/ml TNF-α elicited changes after 72 h. Finally, TNF-α mediated changes in the expression

492 levels of additional NF-κB-dependent genes and genes implicated in NF-κB activation were

493 determined. A robust *BIRC3* (cIAP2) and *TNFAIP3* induction was observed and maintained over

494 time at 100 ng/ml TNF-α. The early significant induction observed at 6 h for *PTGS2* (COX-2)

495   was rapidly decreased after 24 and 72 h. The 10-fold range increase at 6 h observed for *NFKBIA*

496   and *TRAF1* decreased over time at 10 ng/ml TNF-α but was more stable over time at the higher

497   TNF-α dose. Finally, the expression level of the *JUN* component of the transcription factor

498   activator protein-1 (AP-1) was most efficiently increased by 100 ng/ml TNF-α concentrations at

499   later time-points.

500   TNF-α mediated changes were also observed for connective sheets (Table 4). The gene

501   expression of both TNF-α receptors and the prostaglandin E synthases (*PTGES*, *PTGES2*,

502   *PTGES3*) were modulated in a similar fashion than for adipose sheets. The expression levels of

503   NF-κB-dependent genes and genes implicated in NF-κB activation were also upregulated (Table

504   4).

505

506   **Table 4. Gene expression in connective sheets is modulated by TNF-α exposure**

Gene symbol	Fold variation over control [#]					
Treatment duration	6 h		24 h		72 h	
[TNF] (ng/ml)	**10**	**100**	**10**	**100**	**10**	**100**
TNFRSF1A	-1.1	-1.1 *	-1.3 **	-1.4 **	-1.1	-1.6 ***
TNFRSF1B	1.8 *	1.7 **	1.8 **	2.1 ****	1.6 *	4.5 ***
CCL2	4.9 **	4.8 ***	5.1 ***	8.6 ****	2.3 *	9.9 ***
PTGES	3.2 *	3.3 **	4.4 **	6.9 ***	1.3	10.4 **
PTGES2	1.0	1.2	-1.1	-1.1	-1.2	-1.2

28

		*	*			**
PTGES3	1.1	1.0	-1.2 **	-1.1	1.0	-1.0
NFKB1	4.4 ***	4.5 **	2.1 ****	3.5 ****	1.4 *	3.1 **
NFKB2	4.0 **	5.2 **	2.8 ****	4.5 ***	1.7 *	4.9 **
IKBKB	1.5 **	1.5 *	1.1	1.1 **	-1.0	1.2 **
NFKBIA	5.3 ***	6.7 **	4.4 **	8.4 ****	1.8 *	7.6 **
BIRC3	9.8 **	11.2 **	13.3 **	26.7 ***	4.0 *	30.3 **
TNFAIP3	12.1 **	15.5 **	5.0 **	12.8 ***	2.2 *	19.9 **
PTGS2	7.7 *	13.4 *	5.9 *	12.0 ***	1.1	12.9 **
TRAF1	8.1 *	9.5 **	2.9 *	4.8 ****	1.2	3.3 **
JUN	1.4 *	1.5 *	-1.3 ****	-1.2 *	-1.1	-1.1

507   (-) indicates a decrease in expression.

508   [#] Statistical analyses were performed for each time-point using one-sample *t*-tests comparing fold

509   variation ratio of each TNF-α condition to the untreated controls (value of 1). (****$P \leq 0.0001$,

510   ***$P \leq 0.001$, **$P \leq 0.01$, *$P \leq 0.05$).

511

Generating adipocytes at different stages of differentiation

512 Finally, we adapted the culture conditions of our tissue engineering strategy in order to produce a

513

514 wider range of hrAT featuring adipocytes at various stages of the differentiation process. The

515 generic engineering approach consists of inducing adipogenesis after 7 days of culture with AsA,

516 lifting the cell sheets after 28 days of culture, followed by an additional week in culture to favor

517 cohesion between cell sheets before analysis (Fig 5A). We relied on dynamic culture conditions

518 based on the use of a 3D rotator creating a wave-like movement on the engineered cell sheets to

519 circumvent a particularity associated with the production of adipose tissues using the self-

520 assembly method. While long-term ascorbate-stimulated ECM production is needed to ensure the

521 production of manipulatable adipose sheets under static conditions, such ECM, when abundant,

522 also reduces efficient induction of adipogenesis at later stages of culture. This is seen by the 27 %

523 (day 14) and 42 % (day 21, $P \leq 0.05$) reduction of total intracellular lipids quantified after ORO

524 staining on whole adipose sheets cultured for a fixed period of 14 days of differentiation (Fig 5B,

525 Static). The use of a wave-like movement of medium throughout the culture period prevented this

526 loss in lipid accumulation seen when induction is performed later at day 14 or 21 of culture (Fig

527 5B, Dynamic). No impact of the dynamic rotator culture was evidenced when induction was

528 performed at the standard day 7 of culture. Reconstructed tissues produced under dynamic

529 conditions were assessed both as transverse sections after Masson's trichrome staining (Fig 5C,

530 left) and following Oil Red O staining of formol-fixed cryosections (Fig 5C, right). When all

531 tissues are harvested and processed at a specified time-point (after 35 days of culture), numerous

532 small adipocytes representative of earlier stages of differentiation (differentiated for 14 days) can

533 be seen in the hrAT induced at day 21 of culture in comparison to more developed adipocytes

534   differentiated for a period of 21 or 28 days resulting from the adipogenic induction at day 14 and

535   7 of culture respectively (Fig 5C).

536

537   **Fig 5. Engineering of hrAT featuring adipocytes representative of various stages of**

538   **differentiation.** (A) Schematic representation of the induction schemes leading to the production

539   of the hrAT shown in (C). (B) Intracellular lipid quantification following Oil Red O staining of

540   adipose sheets reconstructed according to static or dynamic culture conditions. While the

541   induction of adipogenesis was performed at different times (day 7, 14 or 21) of culture in

542   presence of AsA, Oil Red O staining was carried out after a fixed period of 14 days during which

543   lipid accumulation proceeded. *$P{\leq}0.05$, One-way ANOVA followed by Tukey's post-hoc test;

544    $^{\#\#\#}P = 0.0003$, $^{\&\&}P = 0.0013$, paired *t*-tests between dynamic and static conditions at a given day

545   of induction. (C) Histological cross-sections of hrCT (no adipocytes) and hrAT featuring smaller

546   or more developed adipocytes according to the day at which induction of adipogenesis was

547   performed under dynamic culture conditions. Masson's trichrome staining on paraffin-embedded

548   hrAT samples (left) show the presence of numerous adipocytes (void spaces) and important ECM

549   content (blue), while Oil Red O staining (right) on formol-fixed cryosections reveals the

550   accumulation of intracellular lipids by the developing adipocytes. Bars = 100 μm.

551

Discussion

553   *In vitro* models adequately recapituling key aspects of adipose tissue biology are needed in order

554   to gain novel insights into the functional roles and biological responses of human adipocytes.

555   Primary adipocyte cultures are difficult to establish considering the buoyancy conferred by the

556   large lipid droplets preventing cell attachment to culture surfaces. While ceiling cultures can

557   provide a mean to study adipocytes freshly isolated from various anatomic depots,

558   dedifferentiation of adipocytes into fibroblast-like precursor cells occurs during longer culture

559   period [46, 47]. Direct maintenance of AT fragments *in vitro* in culture media also has limitations

560   including high variability due to limited cell viability over time in culture [28]. It has been

561   reported that AT viability in organotypic culture could be maintained for long periods (up to 4

562   weeks) by incorporating AT fragments (0.5 mm diameter) into gels made of collagen type I [48,

563   49]. In recent years, various tissue engineering strategies combining cells and scaffolding

564   elements have been developed, widening the spectrum of tissue substitutes available for research

565   and forthcoming clinical applications [37]. Engineering of human adipose tissues can be

566   performed according to various strategies based on the use of natural or synthetic biomaterials,

567   hydrogels or collagen gels [50]. Such tridimensional AT substitutes engineered *in vitro* are

568   advantageous over conventional monolayer culture systems, namely because the cells are

569   surrounded by ECM components providing important mechanical and biochemical cues. When

570   scaffolding elements consist of naturally occurring ECM, the tissue-like context that is recreated

571   *in vitro* then closely resemble the *in vivo* microenvironment.

572

573   Our tissue engineering model, which is based on the self-assembly approach, leads to the

574   production of physiologically relevant hrAT devoid of synthetic or exogenous scaffolding

575   elements. These tissues feature a variety of human ECM components including collagen type IV

576   (Fig 1), as well as fibronectin and the structural collagens type I and V [51]. These matrix

577   components are endogenously produced by ascorbate-stimulated cells, assembled and deposited

578   to form cell sheets *in vitro*. The size of the reconstructed tissues can be customized by the

579   superposition of many cell sheets of the chosen surface area. We have previously shown that

580   hrAT express transcripts for key actors of adipogenic differentiation such as PPARγ, LPL and

581 leptin [51]. Moreover, adipocytes within hrAT mediate β-adrenergic receptor stimulated lipolysis

582 under standard culture conditions [39]. At the protein level, leptin is secreted in increasing

583 amounts with cell differentiation, for at least 56 days in culture after adipogenic induction [39].

584 The present study establishes that sizable hrAT can be produced and manipulated with forceps,

585 their prominent stromal compartment providing mechanical support to fragile adipocytes. They

586 were structurally stable over a long culture period while remaining metabolically active. This is

587 particularly relevant considering the degradation rates or remodeling events associated with other

588 types of biomaterials available for soft tissue reconstruction. Although it cannot be excluded that

589 some dedifferentiation events could occur at the cellular level within hrAT over 11 weeks in

590 culture, the Ang-1 secretion profiles, combined with the adipocyte size evaluation, indicate that

591 globally, adipocytes maintained their differentiated features, secretory activity and ability to

592 accumulate triglycerides through *de novo* synthesis over this extended culture period.

593

594 Caution should be used when attempting to compare two different culture systems such as hrAT

595 and AT fragments maintained as organotypic cultures. Nonetheless, parallels can be drawn and

596 the secretion of five important adipokines was established in media conditioned by AT explants

597 and by hrAT featuring adipocytes differentiated for 28 days *in vitro*. Data normalization using

598 total DNA content allowed a partial adjustment for differences in weight and cell numbers among

599 samples, donors and tissue types. Similar amounts of leptin and PAI-1 were detected between AT

600 explants and hrAT, while the latter secreted higher quantities of Ang-1 and VEGF. The very low

601 VEGF content that we quantified in media conditioned by AT explants is consistent with the

602 limited VEGF release measured for AT explants from obese individuals and the predominant

603 VEGF release from nonfat cells [52].

604

605   As previously described for tissue from obese humans, release of adipokines by AT is the result

606   of combined secretion from matrix-resident cells as well as lipid-filled adipocytes [52]. The

607   contribution of *in vitro* differentiated adipocytes to the secreted levels of leptin and Ang-1 is

608   particularly significant when comparing hrAT to connective tissues devoid of adipocytes (hrCT).

609   Our results highlight that the undifferentiated ASCs populating the connective tissues are also

610   active producers of proangiogenic factors such as VEGF and Ang-1, for which sustained levels

611   were detected over an extended time period (at least 49 days). Surprisingly low levels of HGF

612   were detected in media conditioned by hrCT and hrAT in comparison to AT explants. This could

613   suggest that other cell types present in freshly harvested AT explants contribute to HGF levels,

614   such as endothelial cells and macrophages [16, 53].

615

616   Increased adiposity is associated with local inflammation and a dysregulation of adipokine

617   secretion that promotes the development and maintenance of a low-grade proinflammatory state

618   contributing to the establishment of the metabolic syndrome [3]. TNF-α being a potent inducer of

619   adipokine changes, we investigated its impact *in vitro* on reconstructed adipose and connective

620   sheets [20, 54]. The cellular actions of TNF-α are mediated by two receptors for which we

621   validated the presence at the gene expression level. This is in accordance with the TNFRI and

622   TNFRII expression reported on stromal cells and adipocytes of human subcutaneous AT [55].

623   Moreover, the increase in *TNFRSF1B* mRNA levels we observed upon TNF-α stimulation is

624   reminiscent of the increase in TNFRII observed in tissues from obese patients [56]. MCP-1 is

625   produced in high amounts by immune cells such as macrophages which are found in increased

626   numbers in AT from obese patients. This cytokine is also produced by stromal cells and

627   adipocytes, therefore contributing to the AT inflammatory state [57]. Our results using TNF-α-

628   stimulated adipose sheets *in vitro* revealed increased secretion of MCP-1, NGF and HGF

34

629 compared to untreated controls, while no effect on VEGF or leptin levels were observed after a

630 24 h exposure. TNF-α-stimulated connective sheets *in vitro* also revealed an increased secretion

631 of MCP-1 and HGF, highlighting the important contribution of stromal cells. AT explants

632 stimulated with 10 ng/ml TNF-α displayed a secretion profile similar to adipose sheets for MCP-

633 1 and leptin secretion. However, the slight increase in HGF secretion seen for hrAT and hrCT

634 was not observed in these explants, a response that could be masked by the elevated amounts of

635 HGF already produced by the AT explants compared to the reconstructed tissues (10-fold).

636 Collectively, similar effects of TNF-α have been described using either 3T3-L1 adipocytes,

637 human or murine isolated adipocytes or AT explants from lean or obese individuals. In fact,

638 numerous investigations have described the pro-inflammatory effects of TNF-α through increased

639 MCP-1, NGF as well as HGF secretion, although increased VEGF regulation have also been

640 observed [58-61]. Investigations of the interaction between TNF-α and leptin synthesis *in vitro*

641 provided conflicting outcomes, as discussed by Finck and collaborators [62]. While increased

642 leptin expression after TNF-α stimulation is often reported, other studies observed reduced leptin

643 levels in culture [48, 60, 62-64]. These seemingly divergent reports likely arise from the use of

644 various experimental systems and highlight the importance of characterizing each newly

645 developed culture model. Our experiments conducted on human AT explants showed that a dose

646 of 10 ng/ml TNF-α for 24 h did not modify leptin secretion, similarly to the results observed for

647 hrAT. Finally, the 3D microenvironment recreated by the presence of stromal cells and

648 endogenous ECM components surrounding human adipocytes in hrAT greatly contributed to the

649 cellular responses observed.

650

651 While leptin secretion was not modulated by a 24 h TNF-α exposure under these culture

652 conditions, the impact of this cytokine on genes essential for adipocyte metabolic functions

653   including energy uptake and storage was concordant with data reported for 3T3-L1 adipocytes

654   [65]. TNF-α downregulated the expression of genes encoding Glut-4 (*SLC2A4*) and FAS (*FASN*),

655   two proteins that are essential for insulin-mediated uptake of glucose and fatty acid synthesis,

656   respectively. Likewise, *LIPE* expression was also downregulated, which gene encodes HSL

657   mediating the hydrolysis of triglycerides into fatty acids, indicating that TNF-α partly suppresses

658   genes that are essential for metabolic functions of adipocytes, including energy uptake and

659   storage. TNF-α is well known to modulate the expression of many response genes involved in

660   inflammation and energy metabolism through the activation of nuclear factor κB (NF-κB).

661   Importantly, it has been previously shown in 3T3-L1 adipocytes that NF-κB is an obligatory

662   mediator of most of the TNF-α-induced cellular responses, namely using a non-degradable NF-

663   κB inhibitor [65]. Although gene expression studies cannot reveal the expected translocation of

664   the NF-κB factor to the nucleus after TNF-α stimulation, mRNA levels of IκB kinase beta

665   (*IKBKB*) were upregulated in the treated adipose and connective sheets, and could possibly

666   enhance the phosphorylation of IκB at the protein level and the subsequent release and activation

667   of NF-κB. As expected, the gene expression of several components of the NF-κB signalling

668   cascades were upregulated in TNF-α stimulated tissues such as *NFKB1*, *NFKB2* and *NFKBIA*. In

669   addition, mRNA levels of the NFκB target genes *PTGS2, TNFAIP3*, *TRAF1* were significantly

670   modulated in a time-dependent manner. Taken together, these results are suggestive of an NFκB-

671   dependent alteration of AT-associated transcripts and secreted products in our reconstructed

672   tissues.

673

674   The reconstructed tissues we described therefore represent unique tools to investigate in a

675   controlled manner the effects of pharmacologically active products on human differentiated

676   adipocytes as well as compounds modulating adipogenesis from precursor cells. The versatility of

677   our model was further emphasized by the ability to generate tissues featuring human adipocytes

678   at different stages of differentiation. This was achieved using dynamic culture conditions

679   generating a wave-live movement of the media in the culture dishes. Such movement does not

680   impact cell proliferation [41], but could likely increase mass transport and the availability of the

681   adipogenic signal to cells.

682

683   The tissue engineering model we described is particularly useful to investigate the effects of

684   bioactive molecules on adipocytes or stromal cells apart from the influence of other cell types

685   present in native AT. Conversely, it is also possible to sequentially add other cell types to

686   generate more complex tissues. For example, we and others have incorporated endothelial cells

687   into *in vitro* reconstructed adipose tissues, allowing the concomitant evaluation of angiogenic and

688   adipogenic processes [42, 66-68]. Using such a model based on silk biomaterial and spinner

689   flasks cultures, Bellas *et al.* reported the engineering of human adipose tissues maintaining leptin

690   secretion for 24 weeks in culture [68]. In the future, the incorporation of immune cells to

691   engineered models would be highly informative for immuno-adipobiology studies mimicking

692   inflammation.

693

694   In conclusion, we successfully engineered human AT models presenting morphological and

695   functional characteristics closely similar to human AT. In addition to revealing the relatively long

696   stability in culture of these engineered tissues, this study establishes the basal and TNF-α-

697   stimulated secretory capacity of the adipocytes and stromal cells, therefore allowing long-term

698   assessment of metabolic responses *in vitro*. The availability of tissue engineered model systems

699   that are physiologically relevant and recapitulate the complex 3D nature of adipose tissue will

700   likely broaden their use in toxicology screening and drug development studies.

701

Acknowledgements

708

References

710 1.   Berg AH, Scherer PE. Adipose tissue, inflammation, and cardiovascular disease. Circ Res.
711 2005;96(9):939-49. doi: 10.1161/01.RES.0000163635.62927.34.
712 2.   Goralski KB, Sinal CJ. Type 2 diabetes and cardiovascular disease: getting to the fat of
713 the matter. Can J Physiol Pharmacol. 2007;85(1):113-32. doi: 10.1139/y06-092.
714 3.   Ouchi N, Parker JL, Lugus JJ, Walsh K. Adipokines in inflammation and metabolic
715 disease. Nat Rev Immunol. 2011;11(2):85-97. doi: 10.1038/nri2921.
716 4.   Tchernof A, Despres JP. Pathophysiology of human visceral obesity: an update. Physiol
717 Rev. 2013;93(1):359-404. doi: 10.1152/physrev.00033.2011.
718 5.   Kissebah AH, Vydelingum N, Murray R, Evans DJ, Hartz AJ, Kalkhoff RK, et al.
719 Relation of body fat distribution to metabolic complications of obesity. J Clin Endocrinol Metab.
720 1982;54(2):254-60. doi: 10.1210/jcem-54-2-254.
721 6.   Wu J, Bostrom P, Sparks LM, Ye L, Choi JH, Giang AH, et al. Beige adipocytes are a
722 distinct type of thermogenic fat cell in mouse and human. Cell. 2012;150(2):366-76. doi:
723 10.1016/j.cell.2012.05.016.
724 7.   Gesta S, Tseng YH, Kahn CR. Developmental origin of fat: tracking obesity to its source.
725 Cell. 2007;131(2):242-56. doi: 10.1016/j.cell.2007.10.004.
726 8.   Hauner H. Secretory factors from human adipose tissue and their functional role. Proc
727 Nutr Soc. 2005;64(2):163-9.
728 9.   MacLaren R, Cui W, Cianflone K. Adipokines and the immune system: an adipocentric
729 view. Adv Exp Med Biol. 2008;632:1-21.
730 10.   Lumeng CN, Saltiel AR. Inflammatory links between obesity and metabolic disease. J
731 Clin Invest. 2011;121(6):2111-7. doi: 10.1172/JCI57132.
732 11.   Cao Y. Angiogenesis modulates adipogenesis and obesity. J Clin Invest.
733 2007;117(9):2362-8. doi: 10.1172/JCI32239.

734 12. Sierra-Honigmann MR, Nath AK, Murakami C, Garcia-Cardena G, Papapetropoulos A,
735 Sessa WC, et al. Biological action of leptin as an angiogenic factor. Science.
736 1998;281(5383):1683-6.
737 13. Zhang QX, Magovern CJ, Mack CA, Budenbender KT, Ko W, Rosengart TK. Vascular
738 endothelial growth factor is the major angiogenic factor in omentum: mechanism of the
739 omentum-mediated angiogenesis. J Surg Res. 1997;67(2):147-54. doi: 10.1006/jsre.1996.4983.
740 14. Davis S, Aldrich TH, Jones PF, Acheson A, Compton DL, Jain V, et al. Isolation of
741 angiopoietin-1, a ligand for the TIE2 receptor, by secretion-trap expression cloning. Cell.
742 1996;87(7):1161-9.
743 15. Crandall DL, Busler DE, McHendry-Rinde B, Groeling TM, Kral JG. Autocrine
744 regulation of human preadipocyte migration by plasminogen activator inhibitor-1. J Clin
745 Endocrinol Metab. 2000;85(7):2609-14. doi: 10.1210/jcem.85.7.6678.
746 16. Nakamura Y, Morishita R, Higaki J, Kida I, Aoki M, Moriguchi A, et al. Expression of
747 local hepatocyte growth factor system in vascular tissues. Biochem Biophys Res Commun.
748 1995;215(2):483-8.
749 17. Hotamisligil GS. Inflammation and metabolic disorders. Nature. 2006;444(7121):860-7.
750 doi: 10.1038/nature05485.
751 18. Maury E, Brichard SM. Adipokine dysregulation, adipose tissue inflammation and
752 metabolic syndrome. Mol Cell Endocrinol. 2010;314(1):1-16. doi: 10.1016/j.mce.2009.07.031.
753 19. Dandona P, Weinstock R, Thusu K, Abdel-Rahman E, Aljada A, Wadden T. Tumor
754 necrosis factor-alpha in sera of obese patients: fall with weight loss. J Clin Endocrinol Metab.
755 1998;83(8):2907-10. doi: 10.1210/jcem.83.8.5026.
756 20. Sethi JK, Hotamisligil GS. The role of TNF alpha in adipocyte metabolism. Semin Cell
757 Dev Biol. 1999;10(1):19-29. doi: 10.1006/scdb.1998.0273.
758 21. Lafontan M. Historical perspectives in fat cell biology: the fat cell as a model for the
759 investigation of hormonal and metabolic pathways. Am J Physiol Cell Physiol.
760 2012;302(2):C327-59. doi: 10.1152/ajpcell.00168.2011.
761 22. Trayhurn P, Wood IS. Signalling role of adipose tissue: adipokines and inflammation in
762 obesity. Biochem Soc Trans. 2005;33(Pt 5):1078-81. doi: 10.1042/BST20051078.
763 23. Schipper HS, Prakken B, Kalkhoven E, Boes M. Adipose tissue-resident immune cells:
764 key players in immunometabolism. Trends Endocrinol Metab. 2012;23(8):407-15. doi:
765 10.1016/j.tem.2012.05.011.
766 24. Ferrante AW, Jr. The immune cells in adipose tissue. Diabetes Obes Metab. 2013;15
767 Suppl 3:34-8. doi: 10.1111/dom.12154.
768 25. Green H, Meuth M. An established pre-adipose cell line and its differentiation in culture.
769 Cell. 1974;3(2):127-33.
770 26. Green H, Kehinde O. Spontaneous heritable changes leading to increased adipose
771 conversion in 3T3 cells. Cell. 1976;7(1):105-13.
772 27. Mahadik SR, Lele RD, Mehtalia SD, Deo SS, Parikh V. Regulation of adiponectin
773 secretion in human subcutaneous and omental adipose tissue: effects of pioglitazone and
774 endothelin-1: a pilot study. J Assoc Physicians India. 2013;61(4):244-8.
775 28. Gesta S, Lolmede K, Daviaud D, Berlan M, Bouloumie A, Lafontan M, et al. Culture of
776 human adipose tissue explants leads to profound alteration of adipocyte gene expression. Horm
777 Metab Res. 2003;35(3):158-63. doi: 10.1055/s-2003-39070.
778 29. Zuk PA, Zhu M, Mizuno H, Huang J, Futrell JW, Katz AJ, et al. Multilineage cells from
779 human adipose tissue: implications for cell-based therapies. Tissue Eng. 2001;7(2):211-28. doi:
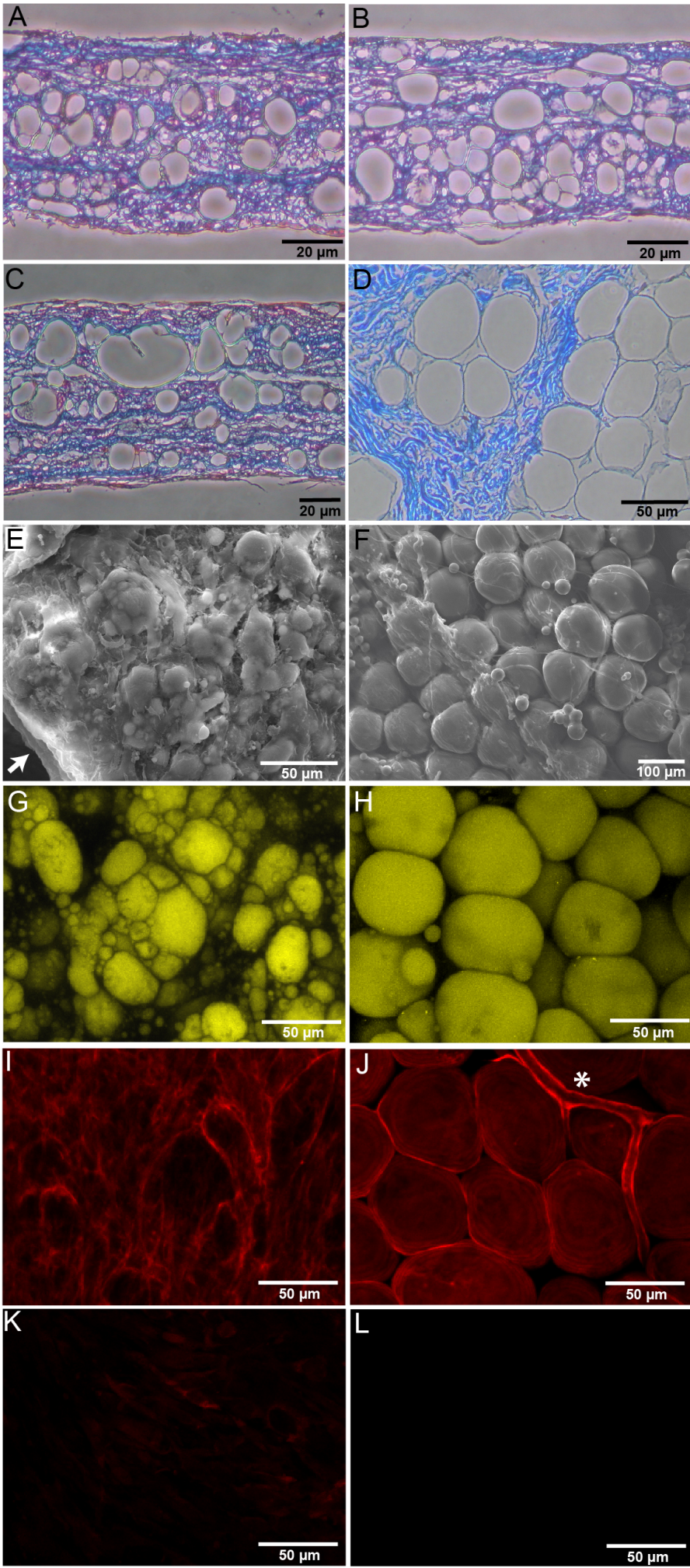780 10.1089/107632701300062859.

781 30.   Lindroos B, Suuronen R, Miettinen S. The potential of adipose stem cells in regenerative
782 medicine. Stem Cell Rev. 2011;7(2):269-91. doi: 10.1007/s12015-010-9193-7.
783 31.   Zuk PA, Zhu M, Ashjian P, De Ugarte DA, Huang JI, Mizuno H, et al. Human adipose
784 tissue is a source of multipotent stem cells. Mol Biol Cell. 2002;13(12):4279-95. doi:
785 10.1091/mbc.E02-02-0105.
786 32.   Tsuji W, Rubin JP, Marra KG. Adipose-derived stem cells: Implications in tissue
787 regeneration. World J Stem Cells. 2014;6(3):312-21. doi: 10.4252/wjsc.v6.i3.312.
788 33.   Murphy MB, Moncivais K, Caplan AI. Mesenchymal stem cells: environmentally
789 responsive therapeutics for regenerative medicine. Exp Mol Med. 2013;45:e54. doi:
790 10.1038/emm.2013.94.
791 34.   Salgado AJ, Reis RL, Sousa NJ, Gimble JM. Adipose tissue derived stem cells secretome:
792 soluble factors and their roles in regenerative medicine. Curr Stem Cell Res Ther. 2010;5(2):103-
793 10.
794 35.   Philips BJ, Marra KG, Rubin JP. Adipose stem cell-based soft tissue regeneration. Expert
795 Opin Biol Ther. 2012;12(2):155-63. doi: 10.1517/14712598.2012.644533.
796 36.   Cukierman E, Pankov R, Stevens DR, Yamada KM. Taking cell-matrix adhesions to the
797 third dimension. Science. 2001;294(5547):1708-12. doi: 10.1126/science.1064829.
798 37.   Griffith LG, Swartz MA. Capturing complex 3D tissue physiology in vitro. Nat Rev Mol
799 Cell Biol. 2006;7(3):211-24. doi: 10.1038/nrm1858.
800 38.   Bauer-Kreisel P, Goepferich A, Blunk T. Cell-delivery therapeutics for adipose tissue
801 regeneration. Adv Drug Deliv Rev. 2010;62(7-8):798-813. doi: 10.1016/j.addr.2010.04.003.
802 39.   Vermette M, Trottier V, Menard V, Saint-Pierre L, Roy A, Fradette J. Production of a
803 new tissue-engineered adipose substitute from human adipose-derived stromal cells.
804 Biomaterials. 2007;28(18):2850-60. doi: 10.1016/j.biomaterials.2007.02.030.
805 40.   Labbe B, Marceau-Fortier G, Fradette J. Cell sheet technology for tissue engineering: the
806 self-assembly approach using adipose-derived stromal cells. In: Gimble JM, Bunnell BA, editors.
807 Methods Mol Biol: Adipose-derived stem cells: methods and protocols. 702. New York: Humana
808 Press; 2011. p. 429-41.
809 41.   Fortier GM, Gauvin R, Proulx M, Vallee M, Fradette J. Dynamic culture induces a cell
810 type-dependent response impacting on the thickness of engineered connective tissues. J Tissue
811 Eng Regen Med. 2013;7(4):292-301. doi: 10.1002/term.522.
812 42.   Aubin K, Vincent C, Proulx M, Mayrand D, Fradette J. Creating capillary networks
813 within human engineered tissues: Impact of adipocytes and their secretory products. Acta
814 Biomater. 2015;11:333-45. doi: 10.1016/j.actbio.2014.09.044.
815 43.   Luu-The V, Paquet N, Calvo E, Cumps J. Improved real-time RT-PCR method for high-
816 throughput measurements using second derivative calculation and double correction.
817 Biotechniques. 2005;38(2):287-93.
818 44.   Fink T, Lund P, Pilgaard L, Rasmussen JG, Duroux M, Zachar V. Instability of standard
819 PCR reference genes in adipose-derived stem cells during propagation, differentiation and
820 hypoxic exposure. BMC Mol Biol. 2008;9:98. doi: 10.1186/1471-2199-9-98.
821 45.   Bustin SA, Benes V, Garson JA, Hellemans J, Huggett J, Kubista M, et al. The MIQE
822 guidelines: minimum information for publication of quantitative real-time PCR experiments. Clin
823 Chem. 2009;55(4):611-22. doi: 10.1373/clinchem.2008.112797.
824 46.   Poloni A, Maurizi G, Leoni P, Serrani F, Mancini S, Frontini A, et al. Human
825 dedifferentiated adipocytes show similar properties to bone marrow-derived mesenchymal stem
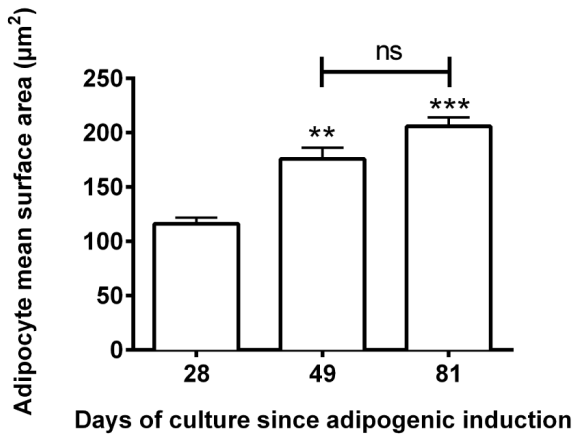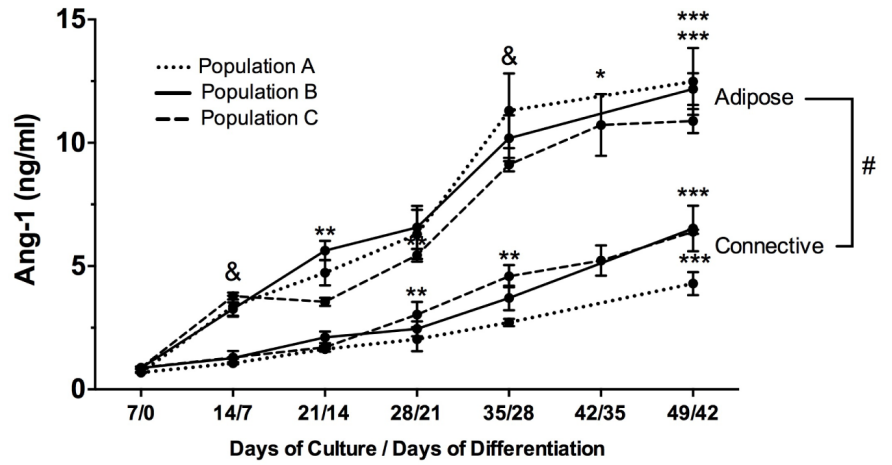826 cells. Stem Cells. 2012;30(5):965-74. doi: 10.1002/stem.1067.

827   47.   Sugihara H, Yonemitsu N, Miyabara S, Yun K. Primary cultures of unilocular fat cells:
828   characteristics of growth in vitro and changes in differentiation properties. Differentiation.
829   1986;31(1):42-9.
830   48.   Sonoda E, Aoki S, Uchihashi K, Soejima H, Kanaji S, Izuhara K, et al. A new
831   organotypic culture of adipose tissue fragments maintains viable mature adipocytes for a long
832   term, together with development of immature adipocytes and mesenchymal stem cell-like cells.
833   Endocrinology. 2008;149(10):4794-8. doi: 10.1210/en.2008-0525.
834   49.   Toda S, Uchihashi K, Aoki S, Sonoda E, Yamasaki F, Piao M, et al. Adipose tissue-
835   organotypic culture system as a promising model for studying adipose tissue biology and
836   regeneration. Organogenesis. 2009;5(2):50-6.
837   50.   Choi JH, Gimble JM, Lee K, Marra KG, Rubin JP, Yoo JJ, et al. Adipose tissue
838   engineering for soft tissue regeneration. Tissue Eng Part B Rev. 2010;16(4):413-26. doi:
839   10.1089/ten.TEB.2009.0544.
840   51.   Vallee M, Cote JF, Fradette J. Adipose-tissue engineering: taking advantage of the
841   properties of human adipose-derived stem/stromal cells. Pathol Biol (Paris). 2009;57(4):309-17.
842   doi: 10.1016/j.patbio.2008.04.010.
843   52.   Fain JN, Madan AK, Hiler ML, Cheema P, Bahouth SW. Comparison of the release of
844   adipokines by adipose tissue, adipose tissue matrix, and adipocytes from visceral and
845   subcutaneous abdominal adipose tissues of obese humans. Endocrinology. 2004;145(5):2273-82.
846   doi: 10.1210/en.2003-1336.
847   53.   Zarnegar R, Michalopoulos GK. The many faces of hepatocyte growth factor: from
848   hepatopoiesis to hematopoiesis. J Cell Biol. 1995;129(5):1177-80.
849   54.   Maury E, Noel L, Detry R, Brichard SM. In vitro hyperresponsiveness to tumor necrosis
850   factor-alpha contributes to adipokine dysregulation in omental adipocytes of obese subjects. J
851   Clin Endocrinol Metab. 2009;94(4):1393-400. doi: 10.1210/jc.2008-2196.
852   55.   Hube F, Birgel M, Lee YM, Hauner H. Expression pattern of tumour necrosis factor
853   receptors in subcutaneous and omental human adipose tissue: role of obesity and non-insulin-
854   dependent diabetes mellitus. Eur J Clin Invest. 1999;29(8):672-8.
855   56.   Good M, Newell FM, Haupt LM, Whitehead JP, Hutley LJ, Prins JB. TNF and TNF
856   receptor expression and insulin sensitivity in human omental and subcutaneous adipose tissue--
857   influence of BMI and adipose distribution. Diab Vasc Dis Res. 2006;3(1):26-33. doi:
858   10.3132/dvdr.2006.003.
859   57.   Gerhardt CC, Romero IA, Cancello R, Camoin L, Strosberg AD. Chemokines control fat
860   accumulation and leptin secretion by cultured human adipocytes. Mol Cell Endocrinol.
861   2001;175(1-2):81-92.
862   58.   Peeraully MR, Jenkins JR, Trayhurn P. NGF gene expression and secretion in white
863   adipose tissue: regulation in 3T3-L1 adipocytes by hormones and inflammatory cytokines. Am J
864   Physiol Endocrinol Metab. 2004;287(2):E331-9. doi: 10.1152/ajpendo.00076.2004.
865   59.   Wang B, Jenkins JR, Trayhurn P. Expression and secretion of inflammation-related
866   adipokines by human adipocytes differentiated in culture: integrated response to TNF-alpha. Am
867   J Physiol Endocrinol Metab. 2005;288(4):E731-40. doi: 10.1152/ajpendo.00475.2004.
868   60.   Wang B, Trayhurn P. Acute and prolonged effects of TNF-alpha on the expression and
869   secretion of inflammation-related adipokines by human adipocytes differentiated in culture.
870   Pflugers Arch. 2006;452(4):418-27. doi: 10.1007/s00424-006-0055-8.
871   61.   Wang M, Crisostomo PR, Herring C, Meldrum KK, Meldrum DR. Human progenitor
872   cells from bone marrow or adipose tissue produce VEGF, HGF, and IGF-I in response to TNF by

873 a p38 MAPK-dependent mechanism. Am J Physiol Regul Integr Comp Physiol.
874 2006;291(4):R880-4. doi: 10.1152/ajpregu.00280.2006.
875 62.   Finck BN, Johnson RW. Anti-inflammatory agents inhibit the induction of leptin by
876 tumor necrosis factor-alpha. Am J Physiol Regul Integr Comp Physiol. 2002;282(5):R1429-35.
877 doi: 10.1152/ajpregu.00569.2001.
878 63.   Kirchgessner TG, Uysal KT, Wiesbrock SM, Marino MW, Hotamisligil GS. Tumor
879 necrosis factor-alpha contributes to obesity-related hyperleptinemia by regulating leptin release
880 from adipocytes. J Clin Invest. 1997;100(11):2777-82. doi: 10.1172/JCI119824.
881 64.   Bruun JM, Pedersen SB, Kristensen K, Richelsen B. Effects of pro-inflammatory
882 cytokines and chemokines on leptin production in human adipose tissue in vitro. Mol Cell
883 Endocrinol. 2002;190(1-2):91-9.
884 65.   Ruan H, Hacohen N, Golub TR, Van Parijs L, Lodish HF. Tumor necrosis factor-alpha
885 suppresses adipocyte-specific genes and activates expression of preadipocyte genes in 3T3-L1
886 adipocytes: nuclear factor-kappaB activation by TNF-alpha is obligatory. Diabetes.
887 2002;51(5):1319-36.
888 66.   Kang JH, Gimble JM, Kaplan DL. In vitro 3D model for human vascularized adipose
889 tissue. Tissue Eng Part A. 2009;15(8):2227-36. doi: 10.1089/ten.tea.2008.0469.
890 67.   Yao R, Du Y, Zhang R, Lin F, Luan J. A biomimetic physiological model for human
891 adipose tissue by adipocytes and endothelial cell cocultures with spatially controlled distribution.
892 Biomed Mater. 2013;8(4):045005. doi: 10.1088/1748-6041/8/4/045005.
893 68.   Bellas E, Marra KG, Kaplan DL. Sustainable Three-Dimensional Tissue Model of Human
894 Adipose Tissue. Tissue Eng Part C Methods. 2013. doi: 10.1089/ten.TEC.2012.0620.
895
896

897

A

Adipocyte mean surface area (µm²)

ns

**

***

28 49 81

Days of culture since adipogenic induction

C

Ang-1 (ng/ml)

······· Population A
——— Population B
‑ ‑ ‑ Population C

&

&

**

**

**

\&

***
***

*

Adipose

#

**

***

Connective

7/0 14/7 21/14 28/21 35/28 42/35 49/42

Days of Culture / Days of Differentiation

B

Frequency distribution (% of total)

30-50 51-100 101-200 201-350 350-1500

28 days of differentiation

Frequency distribution (% of total)

* *

* *

30-50 51-100 101-200 201-350 350-1500

49 days of differentiation

Frequency distribution (% of total)

* *

#
**

30-50 51-100 101-200 201-350 350-1500

81 days of differentiation

Cell surface area (µm²)

A

← Expansion phase → 0   7   14   21   28   35   days of engineering

Seeding ASCs in 6-well plates

Superimposition of cell sheets

Harvest of tissues

Static or Dynamic culture

Induction of adipogenic differentiation

28d of differentiation

Induction of adipogenic differentiation

21d of differentiation

Induction of adipogenic differentiation

14d of differentiation

B

Lipid quantification ORO (Relative units)

*

###

&&

7   14   21   7   14   21

Static   Dynamic

Day of culture at which induction was performed

C

No Induction

Induction at

d7

d14

d21